Published in final edited form as:
Curr Biol. 2013 July 22; 23(14): . doi:10.1016/j.cub.2013.05.035.

Changes in Cell Morphology Are Coordinated with Cell Growth through the TORC1 Pathway

Alexi I. Goranov[1], **Amneet Gulati**[1,2], **Noah Dephoure**[3], **Terunao Takahara**[4], **Tatsuya Maeda**[4], **Steven P. Gygi**[3], **Scott Manalis**[1,2], and **Angelika Amon**[1,5,*]

[1]David H. Koch Institute for Integrative Cancer Research, Massachusetts Institute of Technology, 76-561, 500 Main St., Cambridge, MA 02139, USA

[2]Department of Biological Engineering, Massachusetts Institute of Technology, Cambridge, MA 02139, USA

[3]Department of Cell Biology, Harvard University Medical School, Boston, MA 02115, USA

[4]Institute of Molecular and Cellular Biosciences, The University of Tokyo, 1-1-1 Yayoi, Bunkyo-ku, Tokyo 113-0032, Japan

[5]Howard Hughes Medical Institute

Summary

Background—Growth rate is determined not only by extracellular cues such as nutrient availability but also by intracellular processes. Changes in cell morphology in budding yeast, mediated by polarization of the actin cytoskeleton, have been shown to reduce cell growth.

Results—Here we demonstrate that polarization of the actin cytoskeleton inhibits the highly conserved Target of Rapamycin Complex 1 (TORC1) pathway. This downregulation is suppressed by inactivation of the TORC1 pathway regulatory Iml1 complex, which also regulates TORC1 during nitrogen starvation. We further demonstrate that attenuation of growth is important for cell recovery after conditions of prolonged polarized growth.

Conclusions—Our results indicate that extended periods of polarized growth inhibit protein synthesis, mass accumulation, and the increase in cell size at least in part through inhibiting the TORC1 pathway. We speculate that this mechanism serves to coordinate the ability of cells to increase in size with their biosynthetic capacity.

Introduction

When cells generate more cells (proliferation), they must not only duplicate and segregate their genomic content but also double in size and duplicate macromolecules and cellular organelles (cell growth). How growth and proliferation are coordinated is only partially understood. In most cells, commitment to proliferation depends on growth [1, 2]. The converse relationship—where intracellular proliferative events affect growth—has been described in fission yeast, budding yeast, and mammalian cells [3–5]. Budding yeast G1 cells grow quickly, but as cells enter the cell cycle the growth rate temporarily decreases. The decrease in growth rate coincides with the time when cells are growing in the most

[*]**Correspondence**: angelika@mit.edu.

Supplemental Information

Supplemental Information includes Supplemental Experimental Procedures, six figures, and three tables and can be found with this article online at http://dx.doi.Org/10.1016/j.cub.2013.05.035.

polarized (apical) manner [6, 7]. Polarization of growth is mediated by the asymmetric organization of the actin cytoskeleton (reviewed in [8]). In budding yeast such polarization occurs during bud emergence or mating-projection formation. How polarization of growth by the actin cytoskeleton reduces the growth rate of cells is not known.

Two highly conserved pathways, the RAS and Target of Rapamycin Complex 1 (TORC1) pathways, promote growth in budding yeast (reviewed in [9]). Their activities are primarily affected by nutritional cues. The RAS/PKA pathway is thought to be activated by glucose (reviewed in [9]). The TORC1 pathway, which gets its name from the TOR kinases, is inactivated during nitrogen or amino acid limitation or by various stresses [9, 10]. Budding yeast has two TOR kinases, Tor1 and Tor2, and either can function in the TORC1 complex (reviewed in [10]). TORC1 regulates transcription, translation, and growth through multiple pathways [10]. TORC1 regulates PP2A–like phosphatases [11, 12], transcription factors [13, 14], other kinases [15], and authophagy [16].

Identifying the signals that regulate the TORC1 pathway is essential for understanding how changes in growth, cell proliferation, and cell morphology are coordinated. In mammalian cells, the Rag family of small GTPases controls TORC1 activity in response to nutrient availability [17]. Similarly, Gtr1, a RagA/ B homolog, has been proposed to control TORC1 in budding yeast, at least in part in response to the activity of amino acid tRNA synthetases [18, 19]. In addition, Npr2 and Npr3, which are components of the Iml1 complex [20], are required for proper inhibition of TORC1 during nitrogen depletion [21]. How these factors inhibit TORC1 is not known. Here we show that in budding yeast the status of the actin cytoskeleton, and thus the polarity of growth, regulates TORC1 pathway activity. We find that a polarized actin cytoskeleton inhibits growth and that that this growth inhibition can be partially alleviated by constitutive activation of the TORC1 pathway or by inactivation of the negative regulator of TORC1, the Iml1 complex. We further show that the coordination of growth with changes in cellular morphology is essential for maintaining the ability of cells to resume proliferation after prolonged periods of polarized growth. This link between growth and changes in cell morphology could be a key aspect of the development and survival of highly polarized cells and tissues.

Results

Constitutive Activation of the TORC1 Pathway Partially Suppresses Growth Inhibition Caused by Pheromone Treatment

Our previous studies showed that mating pheromone (α-factor) reduces cell growth through polarization of the actin cytoskeleton [7]. To determine the mechanism whereby this occurs, we first tested whether constitutively active RAS or TORC1 pathways allowed pheromone-treated cells to grow at a faster rate. To this end we used temperature-sensitive *cdc28-4* cells that at the restrictive temperature of 34°C arrest in G1 with a depolarized actin cytoskeleton and a fast growth rate [7]. When pheromone is added to such arrested cells, their growth rate is greatly reduced ([7], Figure 1A; see also Figure S1A in the Supplemental Information available online).

To constitutively activate the RAS/PKA pathway, we employed a constitutive active allele of *RAS2*, *RAS2-V19* [22]. The *RAS2-V19* allele allowed *cdc28-4* arrested cells to grow at an increased rate but did not improve the growth rate of *cdc28-4* cells treated with pheromone (Figure 1A). Hyperactivating the RAS/PKA pathway by deleting *BCY1* produced similar results (Figure S1B). This is best visualized by plotting cell size of pheromone-treated cells as a fraction of the volume of untreated cells (Figure S1C). Our results indicate that the RAS/PKA pathway is not the major target of pheromone-mediated growth inhibition, but they do not exclude the possibility that pheromone treatment affects the RAS/PKA pathway.

Indeed, pheromone treatment causes a reduction in cAMP levels, an indication that the RAS/PKA pathway might be affected [23].

We next tested whether constitutive activation of the TORC1 pathway affected pheromone-mediated downregulation of growth. The recently described hyperactive allele of *TOR1, TOR1-L2134M* [24], did not have a measurable effect on the growth rate of pheromone-treated cells (data not shown). As an alternative approach, we generated a strain that partially mimics constitutively active TORC1 (for a diagram of the TORC1 pathway, see Figure S1D). We combined deletions of the negative regulators of the TORC1 pathway *GAT1*, *GLN3*, and *TIP41* with constitutive alleles of *SFP1* and *SCH9*, the major TORC1 effectors that stimulate protein synthesis and growth [12, 15, 25, 26]. To constitutively activate *SFP1* and *SCH9*, we overexpressed *SFP1* from the *GAL1-10* promoter [25] and introduced a constitutively active allele of *SCH9 (SCH9-2D3E)* [15], respectively. A strain harboring all these alleles (henceforth referred to as TORC1*) grows similarly to wild-type TORC1 cells in the absence of pheromone, at least for the first 4 hr, but noticeably better than cells with wild-type TORC1 in the presence of pheromone (Figures 1B and 1C; see also Figure S1E). This suppression is not due to a defect in the ability of TORC1* strains to respond to pheromone. The TORC1* strain undergoes the pheromone-induced morphological changes with kinetics similar to those of a wild-type strain (Figure S1F). We conclude that pheromone-mediated growth inhibition is partially antagonized by activation of the TORC1 pathway.

Pheromone Treatment Promotes Nuclear Export of Sfp1

Next, we investigated whether TORC1 pathway activity is regulated by pheromone. The transcription factor Sfp1 localizes to the nucleus in nutrient-rich medium to induce expression of ribosomal proteins and the Ribi regulon but is exported from the nucleus under starvation conditions [13, 27]. The TORC1 and the PKA pathways control the localization of Sfp1 [13].

We first arrested cells in G1 by using the ATP analog-sensitive allele *cdc28-as1*. Asynchronously grown *cdc28-as1* cells arrest either as unbudded cells or as budded cells (if they had passed the G1/S transition at the time CDK inhibitor was added [28]). In both cases they arrest with a depolarized actin cytoskeleton and low CDK activity and are responsive to pheromone. We term this a “G1-like” state so that it is inclusive of budded cells. In *cdc28-as1* cells treated with inhibitor for 90 min, Sfp1-GFP predominantly localized to the nucleus (Figure 2A). Pheromone addition did not cause a change in Sfp1 -GFP protein levels (Figure 2B) but did cause Sfp1-GFP to leave the nucleus within 30 min of pheromone treatment (Figures 2A and 2C; see also Figure S2B). This is best seen when the ratio of nuclear to cytoplasmic Sfp1 is quantified (Figures S2A and S2B). Similar results were obtained with cells harboring the temperature-sensitive *cdc28-4* allele and with cells that were not treated with CDK inhibitor but that were treated with pheromone (Figures S2A and S2B). The latter observation indicates that the effects of pheromone on Sfp1-GFP localization are physiologically relevant and not a result of CDK inactivation. In cells treated with pheromone we also observed cellular areas that had increased Sfp1-GFP localization but that did not correspond to the nucleus (Figure 2A white arrows). The identity of these structures is at present unknown.

Because Sfp1 localization is affected by both TORC1 and RAS, we next determined whether modulating RAS/PKA pathway activity affects pheromone-induced Sfp1 nuclear export. We monitored the localization of Sfp1 -GFP in a strain that harbors the constitutively active *RAS2-V19* allele and found that pheromone treatment caused Sfp1 to exit the nucleus in such cells (Figure S2B). We conclude that Sfp1 -GFP localization is affected by

pheromone in a manner consistent with the TORC1 pathway's being inactivated by this treatment.

A careful analysis of the sequence of events following pheromone addition showed that the export of Sfp1 -GFP from the nucleus occurred concomitantly with pheromone-induced polarization of the actin cytoskeleton. Activation of the pheromone-signaling MAP kinases Fus3 and Kss1 occurred within 5 min of pheromone treatment (Figure 2D). Most polarization of the actin cytoskeleton occurred between 15 and 30 min (Figure 2E). Sfp1 exited the nucleus with similar kinetics (Figure 2C). We conclude that nuclear export of Sfp1 closely correlates with pheromone-induced polarization of the actin cytoskeleton.

Pheromone Treatment Affects the Phosphorylation State of TORC1 Pathway Targets

The protein kinase Sch9 is a direct target of TORC1. TORC1 phosphorylates the protein at the C terminus on at least five sites, T723, S726, T737, S758, and S765 [15]. Changes in migration on SDS-PAGE gel as a result of phosphorylation of Sch9 are detectible but subtle when the full-length protein is analyzed (Figure S2C), but chemical cleavage of the protein allows for better resolution of the phosphorylated and unphosphorylated species [15]. Inactivation of TORC1 by rapamycin causes the more slowly migrating phosphorylated forms of Sch9 to decline. Conversely, treatment of cells with the protein-synthesis inhibitor cycloheximide leads to Sch9 hyperphosphorylation, presumably because of the increase in amino acid concentration as a result of the inhibition of protein synthesis ([15]; Figure 2F and Figure S2C, lower panel). Pheromone treatment led to a loss of the more slowly migrating form of Sch9 within 20 min of pheromone addition (Figure 2F).

To further characterize the effects of pheromone on Sch9 phosphorylation, we investigated the phosphorylation status of a specific residue, T737, which is dephosphorylated upon rapamycin treatment [15, 24]. During the course of these experiments, we observed that the CDK inhibitor alone transiently reduced the phosphorylation on T737 of Sch9 even in strains not carrying the inhibitor-sensitive *cdc28-as1* allele (data not shown). The relevance of this observation is not clear. Pheromone treatment did not cause dephosphorylation of T737 as effectively as rapamycin treatment, but it might affect the phosphorylation of T737 only subtly. In contrast, the mobility of full-length Sch9 significantly increased in pheromone-treated cells, consistent with the idea that pheromone treatment affects the overall phosphorylation of Sch9 phospho-sites (Figure 2F; see also Figure S2C). Thus, pheromone treatment probably affects the phosphorylation status of multiple Sch9 residues.

Npr1 is a protein kinase involved in amino acid transport. It is (directly or indirectly) phosphorylated in a TORC1 -dependent manner [12]. Npr1 was dephosphorylated after pheromone treatment (Figure 2G). More quickly migrating forms appeared 20 min after pheromone addition. An extremely quickly migrating species of Npr1 became apparent after ~60 min of growth in the presence of pheromone (Figure 2G) as a result of near complete dephosphorylation of the protein (Figure S2D).

To test whether pheromone-induced Npr1 dephosphorylation is the result of the known Npr1 regulation by TORC1, we deleted *SAP155* and *TIP41*, which encode negative regulators of TORC1 signaling [12]. Deletion of *TIP41* had very little effect on Npr1 dephosphorylation. In contrast, deletion of *SAP155* markedly reduced Npr1 dephosphorylation after pheromone treatment but only slightly dampened the effects of rapamycin (Figure S2E). Inactivating *TIP41* did not enhance the effects of deleting *SAP155* in our genetic background (Figure S2E). The mild effect of *sap155Δ* and *tip41Δ* on rapamycin-induced dephosphorylation is most likely due to the more potent TORC1 inhibition caused by the high concentrations of rapamycin that were used. We were not able to assess the effects of *TAP42* on Npr1 phosphorylation because the *TAP42-11* allele is synthetic lethal with the *cdc28-as1* allele in

our strain background. We conclude that changes in Npr1 mobility in response to pheromone are consistent with changes in TORC1 pathway activity.

Par32 phosphorylation increases in response to downregulation of TORC1 by rapamycin treatment [29]. Pheromone treatment also caused an increase in the phosphorylation of Par32, but to a lesser extent than rapamycin (Figure S2F). Thus, multiple known TORC1 pathway targets undergo changes in their phosphorylation state in response to pheromone treatment.

Finally, we conducted a quantitative phospho-proteomics analysis to assess the effects of pheromone on TORC1 pathway signaling. As expected, we identified increases in the phosphorylation state of 27 proteins involved in pheromone signaling (enrichment of "conjugation" GO terms, $p = 1 \times 10^{-5}$). We also detected changes in the phosphorylation of 187 proteins involved in macromolecular synthesis and growth ("regulation of macromolecular synthesis" GO term enrichment $p = 4.6 \times 10^{-15}$); among these were proteins that are known or proposed TORC1 targets (Table 1; see also Tables S1 and S2). For example, we detected a decrease in phosphorylation of Sch9 at T723, a change that has been reported to occur after rapamycin treatment [15, 30]. Consistent with our analysis of Sch9 T737 phosphorylation, we did not detect a significant change in the phosphorylation state of this residue. We also detected a decrease in phosphorylation of Npr1, consistent with our gel-mobility experiments. Of the 43 proteins identified as TORC1 regulated [29], we obtained phospho-peptides for 34 of them and detected a greater-than-1.5-fold change in phosphorylation for 31 of them. Interestingly, for 21 of these 31 proteins, the effects were in the same direction (increase or decrease of phosphorylation) as previously observed in response to rapamycin treatment. Furthermore, for 12 of the 31 proteins we identified changes in phosphorylation on residues that were also affected by rapamycin treatment (Table 1, bolded sites). In summary, our results indicate that pheromone inhibits TORC1 pathway activity.

Pheromone-Mediated Inhibition of TORC1 Pathway Activity Depends on Polarization of the Actin Cytoskeleton

Polarization of the actin cytoskeleton is responsible for the growth-inhibitory effects of pheromone [7]. We thus tested whether pheromone-mediated TORC1 inhibition is also dependent on the polarization of the actin cytoskeleton. We prevented morphological changes in pheromone-treated cells by deleting the gene encoding the formin Bni1, which is required for the polarization of the actin cytoskeleton [7, 8]. Deletion of *BNI1* alleviated the growth inhibition by pheromone (Figure S3A) and prevented the exit of Sfp1-GFP from the nucleus in response to pheromone treatment (Figures 3A and 3B). Importantly, cells lacking *BNI1* responded normally to rapamycin treatment, as evidenced by the fact that Sfp1 exited the nucleus in the presence of rapamycin (Figure 3A). Deletion of *BNI1* also largely abolished the pheromone-induced dephosphorylation of Sch9 and Npr1 (Figures 3C–3E). We conclude that pheromone treatment inhibits the TORC1 pathway through growth polarization induced by the polarization of the actin cytoskeleton. We furthermore note that unlike in mammals, where the microtubule cytoskeleton affects TORC1 pathway activity [31], microtubule depolymerization did not affect the growth rate in apically or isotropically growing yeast (Figure S3B).

Polarized Growth during Budding Inhibits TORC1 Pathway Activity

Cells defective in the SCF ubiquitin ligase, such as the temperature-sensitive *cdc34-2* mutant, accumulate the B-type cyclin inhibitor Sic1, causing cells to arrest with a 1N DNA content, high G1 cyclin levels, and highly polarized buds [32, 33]. TORC1 pathway activity was also inhibited in this mutant. Sfp1-GFP was found in the cytoplasm in 91% of *cdc34-2*

arrested cells (Figures 4A–4C). Overexpression of *SIC1* revealed similar results (data not shown). Furthermore, Sch9 was dephosphorylated in *cdc34-2* cells but less so in *cdc34-2* cells, in which polarization of the actin cytoskeleton was prevented by the inhibition of CDK activity (Figure 4D). We conclude that polarization of growth by the actin cytoskeleton inhibits TORC1 activity not only in response to pheromone treatment but also during apical bud growth.

The Iml1 Complex Affects Growth Inhibition in Response to Polarized Growth

How does polarization of growth inhibit TORC1 pathway activity? Several regulators of the TORC1 pathway have been described in yeast. The GTPase Rho1, activated by its GEF Rom2, inhibits the TORC1 pathway [34]. *rom2*Δ cells grew faster than wild-type cells when arrested in G1 but responded to pheromone treatment in the same manner as wild-type cells (Figures S4A and S4B). Gtr1 and Gtr2 also regulate TORC1 [18]. A *GTR1* mutant that mimics the GTP-bound state of the protein *(GTR1-Q65L)* increases TORC1 activity during amino acid limitation, a condition that normally inactivates TORC1 [18]. Although expression of the *GTR1-Q65L* allele caused cells to grow more slowly, it nevertheless subtly improved the ability of cells to grow in the presence of pheromone (Figures S4C and S4D).

The Iml1 complex negatively regulates TORC1 pathway activity [21]. Deletion of the genes encoding the Iml1 complex components Iml1, Npr2, or Npr3 had very little effect on the growth of G1 -arrested cells but caused a significant improvement in the ability of G1-arrested cells to grow in the presence of pheromone (Figure 5A). Combining *NPR2* and *IML1* deletions did not lead to better growth than each single deletion (Figure S5), indicating that the proteins function in the same pathway. Importantly, inactivation of the Iml1 complex did not interfere with pheromone signaling or polarization of the actin cytoskeleton. Phosphorylation of the pheromone-induced MAP kinases Fus3 and Kss1 and actin polarization were the same in *IML1* and *iml1Δ* cells (Figures 5B and 5C). Thus, the Iml1 complex acts either downstream of or in parallel to polarized growth to affect TORC1 pathway function.

Next, we wanted to corroborate our cell-volume measurements by an alternative technique. We employed the SMR (suspended microchannel resonator [35]) to measure the buoyant mass of single cells. In this particular experiment the *cdc28-4 iml1Δ* double mutant grew slightly more slowly than the *cdc28-4* single mutant, as observed from cell volume (data not shown) and buoyant mass (Figures 5D and 5E; untreated samples). However, pheromone treatment reduced the buoyant mass of *cdc28-4* cells to a greater extent than it reduced that of *cdc28-4 iml1Δ* cells (Figures 5D and 5E). We conclude that the Iml1 complex is required for pheromone-induced growth inhibition.

The Iml1 complex also affects TORC1 inhibition caused by hyperpolarization of the actin cytoskeleton during budding. Deleting *IML1* improved the growth of both *GAL-SIC1* and *cdc53-1* mutant cells (Figures 6A and 6B). The Iml1 complex component Npr2 is an SCF target [36]. The slow-growth phenotype of SCF mutants could thus have been due to Npr2 accumulation rather than to a hyperpolarized actin cytoskeleton. This was not the case, however. Preventing the polarization of growth either by the introduction of a conditional *cdc42-6* allele (Cdc42 is required for polarization of the actin cytoskeleton [8]) or by CDK inactivation caused SCF mutants cells to grow as fast as *cdc42-6* or CDK single mutants, respectively (Figures S5B and S5C). We conclude that the Iml1 complex is required for growth inhibition in response to the polarization of growth by the actin cytoskeleton.

The Iml1 Complex Affects How TORC1 Pathway Activity Is Modulated in Response to Pheromone

Next we determined whether deleting *IML1* modulates how TORC1 pathway activity responds to pheromone. Upon pheromone addition, Sfp1 -GFP exit from the nucleus was delayed and occurred less efficiently in *iml1Δ* cells than in wild-type cells (Figure 6C). Deletion of *IML1* also delayed the dephos-phorylation of Sch9 after pheromone treatment (Figure 6D). It is worth noting that there seems to be more phosphorylated Sch9 (upper band) in the *iml1Δ* mutant prior to pheromone addition (Figure 6D, time 0 min), indicating that the Iml1 complex might be a general inhibitor of TORC1, although *IML1* deletion does not suppress all methods of inactivating TORC1, e.g., rapamycin or very high temperature [21, 24]. We conclude that the Iml1 complex is required for pheromone-mediated inactivation of the TORC1 pathway.

Reduction of Growth during Polarization Promotes Cell Recovery from Pheromone Arrest

We hypothesized that the restriction of growth during mating-projection formation could be important for promoting recovery after prolonged pheromone arrest as the result of a failed mating. To address this possibility, we examined the ability of cells to return to vegetative growth after a 6 hr pheromone exposure. Pheromone treatment improved the ability of *cdc28-4* cells to form colonies after removal of the G1 block (Figures 6E and 6F). The improved capacity to resume proliferation depended on the polarization of the actin cytoskeleton because deleting *BNI1* prevented the pheromone-induced cell survival of *cdc28-4* G1-arrested cells (Figure 6E). Deleting *IML 1* had similar effects (Figure 6F). The effects of deleting *IML1* or *BNI1* were not due to changes in the ability of cells to reenter the cell cycle after the pheromone arrest, as evidenced by the fact that both mutants resumed budding after pheromone removal with kinetics similar to those of *cdc28-4* single mutants (Figure S6). Thus, defects in cell-cycle processes after budding are most likely responsible for the proliferation defects of large cells. Our observations indicate that reducing the growth capacity of pheromone-arrested cells is critical for maintaining the ability of cells to resume proliferation when mating fails.

Discussion

Prolonged apical growth, caused by the polarization of the actin cytoskeleton, leads to a downregulation of cell-mass accumulation. The inhibition of growth is alleviated either by mutations that mimic active TORC1 or by mutations in Iml1 complex, the negative regulator of the TORC1 pathway. None of the individual alleles comprising the TORC1* mutant can alone suppress the growth-inhibitory effects of pheromone, indicating that the observed decrease in growth is caused by the inactivation of many, if not all, downstream TORC1 effectors. It is also important to note that neither TORC1* nor mutations in the Iml1 complex suppress the growth-inhibitory effects of the polarization of growth as completely as deleting *BNI1*. We propose that in addition to inactivating TORC1, polarization of growth limits the ability of cells to grow in size simply by restricting the surface area available for vesicle fusion (see below). Our observations support the hypothesis that TORC1 integrates multiple inputs, including nutritional status and the status of intracellular events and processes, such as changes in cell morphology, and that it coordinates them with growth rate.

Coordination of Cell-Cycle Transitions and TORC1 Pathway Activity—The Geometric-Restriction Model

The increase in cell size of eukaryotic cells is mediated by lipid vesicles traveling on actin cables in yeast, and on microtubules in mammals, and fusion of these vesicles with the plasma membrane [8]. During G1, vesicle deposition occurs throughout the cell as actin

cables are evenly dispersed, and macromolecule biosynthesis occurs at an accordingly high rate. When vesicle deposition is restricted to a small cell surface area, as occurs during highly polarized or apical growth, macromolecule synthesis must be attenuated accordingly; otherwise, too many vesicles would start to accumulate within the cell. Indeed, vesicle build-up has previously been reported to occur early in pheromone-treated or small budded cells, and the accumulation dissipates with time [37, 38]. Our results indicate that cells coordinate cell-surface growth and macromolecule biosynthesis by making TORC1 pathway activity responsive to the status of the actin cytoskeleton. We speculate that when vesicles build up due to growth restriction during polarized growth, the TORC1 pathway is inactivated so that cells can match protein synthesis and membrane expansion. Two observations support this idea. Mutations in the secretion machinery cause a dramatic downregulation of the expression of ribosomal proteins [39], an effect similar to TORC1 inhibition [15]. Furthermore, treatment of cells with the secretion inhibitor Brefeldin A causes Sfp1 to exit from the nucleus [13], an effect consistent with TORC1 and/or PKA inhibition. It is important to note that lack of an intact actin cytoskeleton is not equivalent to isotropic growth because vesicle transport requires actin cables. Indeed, treatment of cells with the actin-depolymerizing drug Latrunculin A or the expression of a dominant-negative form of the actin motor Myo2 strongly inhibits increases in cell size [7, 40].

During an unperturbed cell cycle the transient decrease in vesicle secretion and volume growth at the time of budding [6, 7] might be too short lived to cause a dramatic downregulation of protein synthesis. This could explain why fluctuations in protein synthesis have not been previously observed with synchronized cells or in single-cell assays [41–43]. If protein synthesis is not attenuated during bud emergence, a temporary uncoupling of macromolecule biosynthesis and cell-surface expansion should ensue, resulting in a transient increase in cell density at the time of budding. Indeed, multiple groups have observed this predicted variation in cell density during the cell cycle [44, 45]. We propose that the regulation of TORC1 by polarized growth might be a feedback mechanism that keeps membrane growth and protein synthesis in balance. During an unperturbed cell cycle a brief uncoupling of cell-surface growth and bulk macromolecular biosynthesis can occur without great impact on cell survival. However, when actin cytoskeleton polarization is prolonged, as occurs during pheromone arrest or when the morphogenesis checkpoint is activated, TORC1 pathway activity must be attenuated. Indeed, when this feedback mechanism is disrupted, as in cells lacking *BNI1* or *IML1*, cells lose the ability to resume proliferation after prolonged pheromone arrest (Figure 6F).

How does the actin cytoskeleton affect TORC1 activity? It is possible that actin cables nucleated by formins or that formins themselves directly impact TORC1 activity, but we consider an indirect mode of regulation to be more likely. Genetic screens have firmly linked TORC1 to vesicle trafficking [13, 46]. The TORC1 activator and RagA/B homolog Gtr1 promotes vesicle traffic to the plasma membrane [18, 47]. The Iml1 complex is thought to share homology with the HOPS and CORVET complexes, which are involved in vesicle trafficking to and from the vacuole [20]. We speculate that the TORC1 pathway could be sensitive to the dynamics of vesicle traffic within the cell. Because vesicle movement depends on actin dynamics, we propose that the polarization of the actin cytoskeleton impacts TORC1 activity indirectly by affecting vesicle-movement dynamics and/or direction.

The TORC1 Pathway Response Is Tailored to the Input

Previous studies have established that nitrogen starvation impacts TORC1 signaling differently than treatment with rapamycin. *TOR1* alleles that cause resistance to rapamycin *(TOR1-1)* are still responsive to starvation [48]. Conversely, starvation-resistant mutants,

such as *npr2Δ* and *npr3Δ* mutants, are still sensitive to rapamycin [21]. Even different types of nitrogen-starvation regimes elicit different responses from the TORC1 pathway [26]. The TORC1 pathway's response to the polarization of growth shares features with the nitrogen-starvation response: it causes Sfp1 to exit the nucleus and Sch9 and Npr1 to become dephosphorylated in an *IML1* -dependent manner. However, in contrast to nitrogen starvation, only a fraction of Npr1 is completely dephosphorylated in response to pheromone-induced polarization of growth. One interpretation of these findings is that different treatments might inhibit TORC1 to different degrees, i.e., that the difference is merely quantitative. We favor the idea that the TORC1 responses are qualitatively different. One example that supports this hypothesis is that Pat1 was dephosphorylated in response to rapamycin treatment on Ser457 [29], but was more phosphorylated on the same residue in response to pheromone treatment.

Growth polarization mediated by changes in the cytoskeleton determines a cell's shape and is thus an integral aspect of the biology of many cell types and tissues. Interestingly, another TOR complex, TORC2, regulates actin polarization, largely by regulating sphingolipid biosynthesis. The crosstalk between the two TORC complexes remains to be described, but it will be an interesting venue for future investigation. Given the high degree of conservation of basic cellular processes among all eukaryotes, we suspect that changes in cell growth patterns during morphogenesis will affect macromolecule biosynthesis by modulating TORC1 pathway activity and will thus be a universal aspect of growth control in eukaryotes.

Experimental Procedures

Strain Construction and Growth Conditions

All strains used are derivatives of W303 and are listed in Table S3. Gene deletions and epitope tags were generated by a single step gene replacement method [49]. Growth conditions are indicated in the figure legends.

Methods

Volume increase of arrested cells was measured as previously described [7]. Western blots were performed as described in Goronov et al. [7] but with modifications. Measurements of cell buoyant mass were performed as described in Burg et al. [35] but with modifications. Detailed procedures are described in the Supplemental Information.

Supplementary Material

Refer to Web version on PubMed Central for supplementary material.

Acknowledgments

We thank Robbie Loewith for useful discussion and reagents. We thank Erik Spear, Frank Solomon, and members of the Amon lab for comments and discussions. This work was supported by a postdoctoral fellowship from the American Cancer Society to A.I.G. A.A is an investigator of the Howard Hughes Medical Institute. A.G., S.M., A.I.G., and A.A. are supported by a contract (U54CA143874) from the Physical Sciences Oncology Center at the National Cancer Institute. S.P.G. and N.D. are supported by grants from the National Institutes of Health to S.P.G. (HG003456 and GM067945). T. M. is supported by a Grant-in-Aid for Challenging Exploratory Research (KAKENHI 23651233) from the Japan Society for the Promotion of Science (JSPS) and by a grant from the Uehara Memorial Foundation.

References

1. Jorgensen P, Tyers M. How cells coordinate growth and division. Curr. Biol. 2004; 14:R1014–R1027. [PubMed: 15589139]

2. Haeusser DP, Levin PA. The great divide: coordinating cell cycle events during bacterial growth and division. Curr. Opin. Microbiol. 2008; 11:94–99. [PubMed: 18396093]
3. Mitchison JM, Nurse P. Growth in cell length in the fission yeast Schizosaccharomyces pombe. J. Cell Sci. 1985; 75:357–376. [PubMed: 4044680]
4. Tzur A, Kafri R, LeBleu VS, Lahav G, Kirschner MW. Cell growth and size homeostasis in proliferating animal cells. Science. 2009; 325:167–171. [PubMed: 19589995]
5. Wilker EW, van Vugt MA, Artim SA, Huang PH, Petersen CP, Reinhardt HC, Feng Y, Sharp PA, Sonenberg N, White FM, Yaffe MB. 14–3–3sigma controls mitotic translation to facilitate cytokinesis. Nature. 2007; 446:329–332. [PubMed: 17361185]
6. Mitchison JM. The growth of single cells. II. Saccharomyces cerevisiae. Exp. Cell Res. 1958; 15:214–221. [PubMed: 13574174]
7. Goranov AI, Cook M, Ricicova M, Ben-Ari G, Gonzalez C, Hansen C, Tyers M, Amon A. The rate of cell growth is governed by cell cycle stage. Genes Dev. 2009; 23:1408–1422. [PubMed: 19528319]
8. Pruyne D, Legesse-Miller A, Gao L, Dong Y, Bretscher A. Mechanisms of polarized growth and organelle segregation in yeast. Annu. Rev. Cell Dev. Biol. 2004; 20:559–591. [PubMed: 15473852]
9. Zaman S, Lippman SI, Zhao X, Broach JR. How Saccharomyces responds to nutrients. Annu. Rev. Genet. 2008; 42:27–81. [PubMed: 18303986]
10. Loewith R, Hall MN. Target of rapamycin (TOR) in nutrient signaling and growth control. Genetics. 2011; 189:1177–1201. [PubMed: 22174183]
11. Di Como CJ, Arndt KT. Nutrients, via the Tor proteins, stimulate the association of Tap42 with type 2A phosphatases. Genes Dev. 1996; 10:1904–1916. [PubMed: 8756348]
12. Jacinto E, Guo B, Arndt KT, Schmelzle T, Hall MN. TIP41 interacts with TAP42 and negatively regulates the TOR signaling pathway. Mol. Cell. 2001; 8:1017–1026. [PubMed: 11741537]
13. Singh J, Tyers M. A Rab escort protein integrates the secretion system with TOR signaling and ribosome biogenesis. Genes Dev. 2009; 23:1944–1958. [PubMed: 19684114]
14. Beck T, Hall MN. The TOR signalling pathway controls nuclear localization of nutrient-regulated transcription factors. Nature. 1999; 402:689–692. [PubMed: 10604478]
15. Urban J, Soulard A, Huber A, Lippman S, Mukhopadhyay D, Deloche O, Wanke V, Anrather D, Ammerer G, Riezman H, et al. Sch9 is a major target of TORC1 in Saccharomyces cerevisiae. Mol Cell. 2007; 26:663–674. [PubMed: 17560372]
16. Kamada Y, Yoshino K, Kondo C, Kawamata T, Oshiro N, Yonezawa K, Ohsumi Y. Tor directly controls the Atg1 kinase complex to regulate autophagy. Mol. Cell Biol. 2010; 30:1049–1058. [PubMed: 19995911]
17. Sancak Y, Peterson TR, Shaul YD, Lindquist RA, Thoreen CC, Bar-Peled L, Sabatini DM. The Rag GTPases bind raptor and mediate amino acid signaling to mTORC1. Science. 2008; 320:1496–1501. [PubMed: 18497260]
18. Binda M, Péli-Gulli MP, Bonfils G, Panchaud N, Urban J, Sturgill TW, Loewith R, De Virgilio C. The Vam6 GEF controls TORC1 by activating the EGO complex. Mol. Cell. 2009; 35:563–573. [PubMed: 19748353]
19. Bonfils G, Jaquenoud M, Bontron S, Ostrowicz C, Ungermann C, De Virgilio C. Leucyl-tRNA synthetase controls TORC1 via the EGO complex. Mol. Cell. 2012; 46:105–110. [PubMed: 22424774]
20. Dokudovskaya S, Waharte F, Schlessinger A, Pieper U, Devos DP, Cristea IM, Williams R, Salamero J, Chait BT, Sali A, et al. A conserved coatomer-related complex containing Sec13 and Seh1 dynamically associates with the vacuole in Saccharomyces cerevisiae. Mol. Cell. Proteomics. 2011; 10:M110. 006478. [PubMed: 21454883]
21. Neklesa TK, Davis RW. A genome-wide screen for regulators of TORC1 in response to amino acid starvation reveals a conserved Npr2/3 complex. PLoS Genet. 2009; 5:e1000515. [PubMed: 19521502]
22. Kataoka T, Powers S, McGill C, Fasano O, Strathern J, Broach J, Wigler M. Genetic analysis of yeast RAS1 and RAS2 genes. Cell. 1984; 37:437–145. [PubMed: 6327067]
23. Liao H, Thorner J. Yeast mating pheromone alpha factor inhibits adenylate cyclase. Proc. Natl. Acad. Sci. USA. 1980; 77:1898–1902. [PubMed: 6246513]

24. Takahara T, Maeda T. Transient sequestration of TORC1 into stress granules during heat stress. Mol Cell. 2012; 47:242–252. [PubMed: 22727621]
25. Jorgensen P, Nishikawa JL, Breitkreutz BJ, Tyers M. Systematic identification of pathways that couple cell growth and division in yeast. Science. 2002; 297:395–400. [PubMed: 12089449]
26. Crespo JL, Powers T, Fowler B, Hall MN. The TOR-controlled transcription activators GLN3, RTG1, and RTG3 are regulated in response to intracellular levels of glutamine. Proc. Natl. Acad. Sci. USA. 2002; 99:6784–6789. [PubMed: 11997479]
27. Marion RM, Regev A, Segal E, Barash Y, Koller D, Friedman N, O'Shea EK. Sfp1 is a stress- and nutrient-sensitive regulator of ribosomal protein gene expression. Proc. Natl. Acad. Sci. USA. 2004; 101:14315–14322. [PubMed: 15353587]
28. Bishop AC, Ubersax JA, Petsch DT, Matheos DP, Gray NS, Blethrow J, Shimizu E, Tsien JZ, Schultz PG, Rose MD, et al. A chemical switch for inhibitor-sensitive alleles of any protein kinase. Nature. 2000; 407:395–401. [PubMed: 11014197]
29. Huber A, Bodenmiller B, Uotila A, Stahl M, Wanka S, Gerrits B, Aebersold R, Loewith R. Characterization of the rapamycin-sensitive phosphoproteome reveals that Sch9 is a central coordinator of protein synthesis. Genes Dev. 2009; 23:1929–1943. [PubMed: 19684113]
30. Soulard A, Cremonesi A, Moes S, Schütz F, Jenö P, Hall MN. The rapamycin-sensitive phosphoproteome reveals that TOR controls protein kinase A toward some but not all substrates. Mol. Biol. Cell. 2010; 21:3475–3486. [PubMed: 20702584]
31. Korolchuk VI, Saiki S, Lichtenberg M, Siddiqi FH, Roberts EA, Imarisio S, Jahreiss L, Sarkar S, Futter M, Menzies FM, et al. Lysosomal positioning coordinates cellular nutrient responses. Nat. Cell Biol. 2011; 13:453–160. [PubMed: 21394080]
32. Tyers M. The cyclin-dependent kinase inhibitor p40SIC1 imposes the requirement for Cln G1 cyclin function at start. Proc. Natl. Acad. Sci. USA. 1996; 93:7772–7776. [PubMed: 8755551]
33. Lew DJ, Reed SI. Morphogenesis in the yeast cell cycle: regulation by Cdc28 and cyclins. J. Cell Biol. 1993; 120:1305–1320. [PubMed: 8449978]
34. Yan G, Lai Y, Jiang Y. The TOR complex 1 is a direct target of Rho1 GTPase. Mol. Cell. 2012; 45:743–753. [PubMed: 22445487]
35. Burg TP, Godin M, Knudsen SM, Shen W, Carlson G, Foster JS, Babcock K, Manalis SR. Weighing of biomolecules, single cells and single nanoparticles in fluid. Nature. 2007; 446:1066–1069. [PubMed: 17460669]
36. Spielewoy N, Guaderrama M, Wohlschlegel JA, Ashe M, Yates JR, Wittenberg C 3rd. Npr2, yeast homolog of the human tumor suppressor NPRL2, is a target of Grr1 required for adaptation to growth on diverse nitrogen sources. Eukaryot. Cell. 2010; 9:592–601. [PubMed: 20154027]
37. Baba M, Baba N, Ohsumi Y, Kanaya K, Osumi M. Three-dimensional analysis of morphogenesis induced by mating pheromone alpha factor in Saccharomyces cerevisiae. J. Cell Sci. 1989; 94:207–216. [PubMed: 2695529]
38. Mulholland J, Preuss D, Moon A, Wong A, Drubin D, Botstein D. Ultrastructure of the yeast actin cytoskeleton and its association with the plasma membrane. J. Cell Biol. 1994; 725:381–391. [PubMed: 8163554]
39. Mizuta K, Warner JR. Continued functioning of the secretory pathway is essential for ribosome synthesis. Mol. Cell Biol. 1994; 14:2493–2502. [PubMed: 8139552]
40. Karpova TS, Reck-Peterson SL, Elkind NB, Mooseker MS, Novick PJ, Cooper JA. Role of actin and Myo2p in polarized secretion and growth of Saccharomyces cerevisiae. Mol. Biol Cell. 2000; 11:1727–1737. [PubMed: 10793147]
41. Elliott SG, Warner JR, McLaughlin CS. Synthesis of ribosomal proteins during the cell cycle of the yeast Saccharomyces cerevisiae. J. Bacteriol. 1979; 737:1048–1050. [PubMed: 370092]
42. Woldringh CL, Huls PG, Vischer NO. Volume growth of daughter and parent cells during the cell cycle of Saccharomyces cerevisiae a/alpha as determined by image cytometry. J. Bacteriol. 1993; 775:3174–3181. [PubMed: 8491731]
43. Di Talia S, Skotheim JM, Bean JM, Siggia ED, Cross FR. The effects of molecular noise and size control on variability in the budding yeast cell cycle. Nature. 2007; 448:947–951. [PubMed: 17713537]

44. Bryan AK, Goranov A, Amon A, Manalis SR. Measurement of mass, density, and volume during the cell cycle of yeast. Proc. Natl. Acad. Sci. USA. 2010; 107:999–1004. [PubMed: 20080562]

45. Hartwell LH. Periodic density fluctuation during the yeast cell cycle and the selection of synchronous cultures. J. Bacteriol. 1970; 104:1280–1285. [PubMed: 16559104]

46. Zurita-Martinez SA, Puria R, Pan X, Boeke JD, Cardenas ME. Efficient Tor signaling requires a functional class C Vps protein complex in Saccharomyces cerevisiae. Genetics. 2007; 176:2139–2150. [PubMed: 17565946]

47. Gao M, Kaiser CA. A conserved GTPase-containing complex is required for intracellular sorting of the general amino-acid permease in yeast. Nat. Cell Biol. 2006; 8:657–667. [PubMed: 16732272]

48. Jorgensen P, Rupes I, Sharom JR, Schneper L, Broach JR, Tyers M. A dynamic transcriptional network communicates growth potential to ribosome synthesis and critical cell size. Genes Dev. 2004; 18:2491–2505. [PubMed: 15466158]

49. Longtine MS, McKenzie A, Demarini DJ 3rd, Shah NG, Wach A, Brachat A, Philippsen P, Pringle JR. Additional modules for versatile and economical PCR-based gene deletion and modification in Saccharomyces cerevisiae. Yeast. 1998; 14:953–961. [PubMed: 9717241]

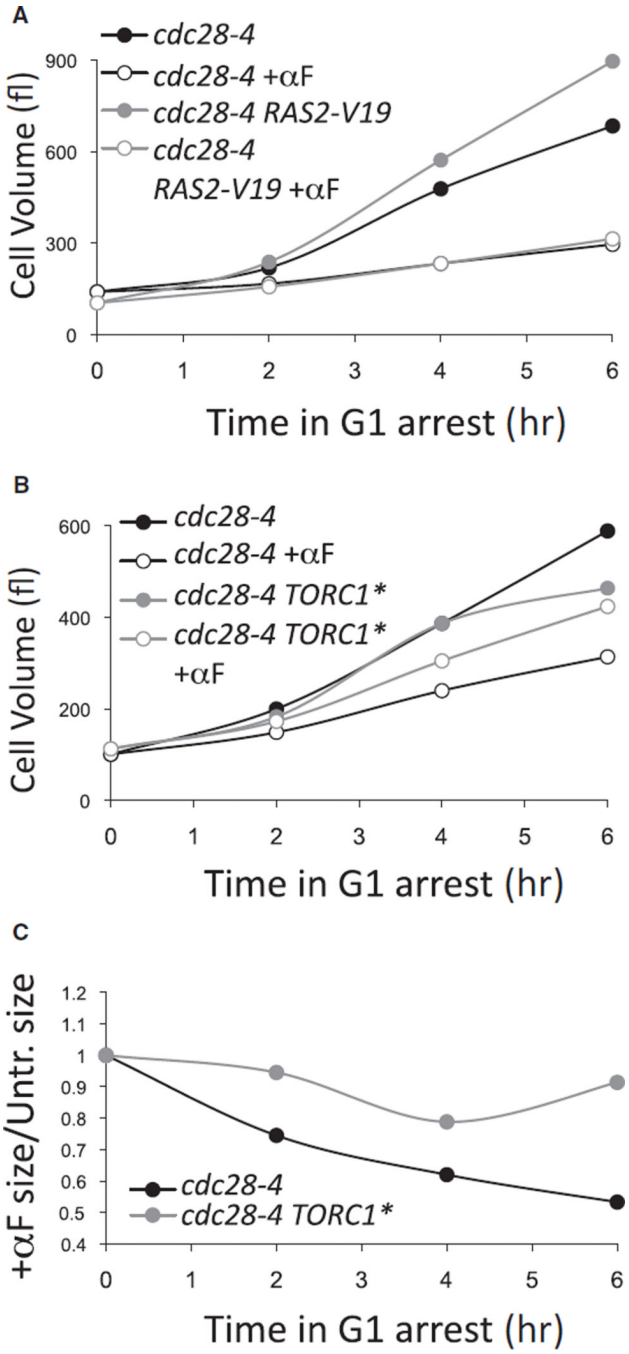

Figure 1. Constitutive Activation of the TORC1 Pathway but Not the RAS/PKA Pathway Improves Cell Growth in the Presence of Mating Pheromone

(A) *cdc28-4* (A17132, black lines) and *cdc28-4 RAS2-V19* (A31570, gray lines) cells grown in YEPD were shifted to 34°C to be arrested in G1. Immediately after temperature shift, the cultures were split. One half were left untreated (filled symbols), and one half were treated with mating pheromone (+αF; 20 μg/ml; open symbols). At the indicated time points, cell volumes were measured so that growth could be assessed.

(B) *cdc28-4* (A17132) and *cdc28-4 TORC1** (A33018) cells were treated as in (A), except that cells were grown in YEP + 2% raffinose and that 1 % galactose was added 1 hr prior to

the shift to 34°C. Note that growth in raffinose and galactose causes a reduction in growth rate.

(C) The data from (B) are plotted as the ratio of the size of pheromone-treated cells to the size of the untreated samples.

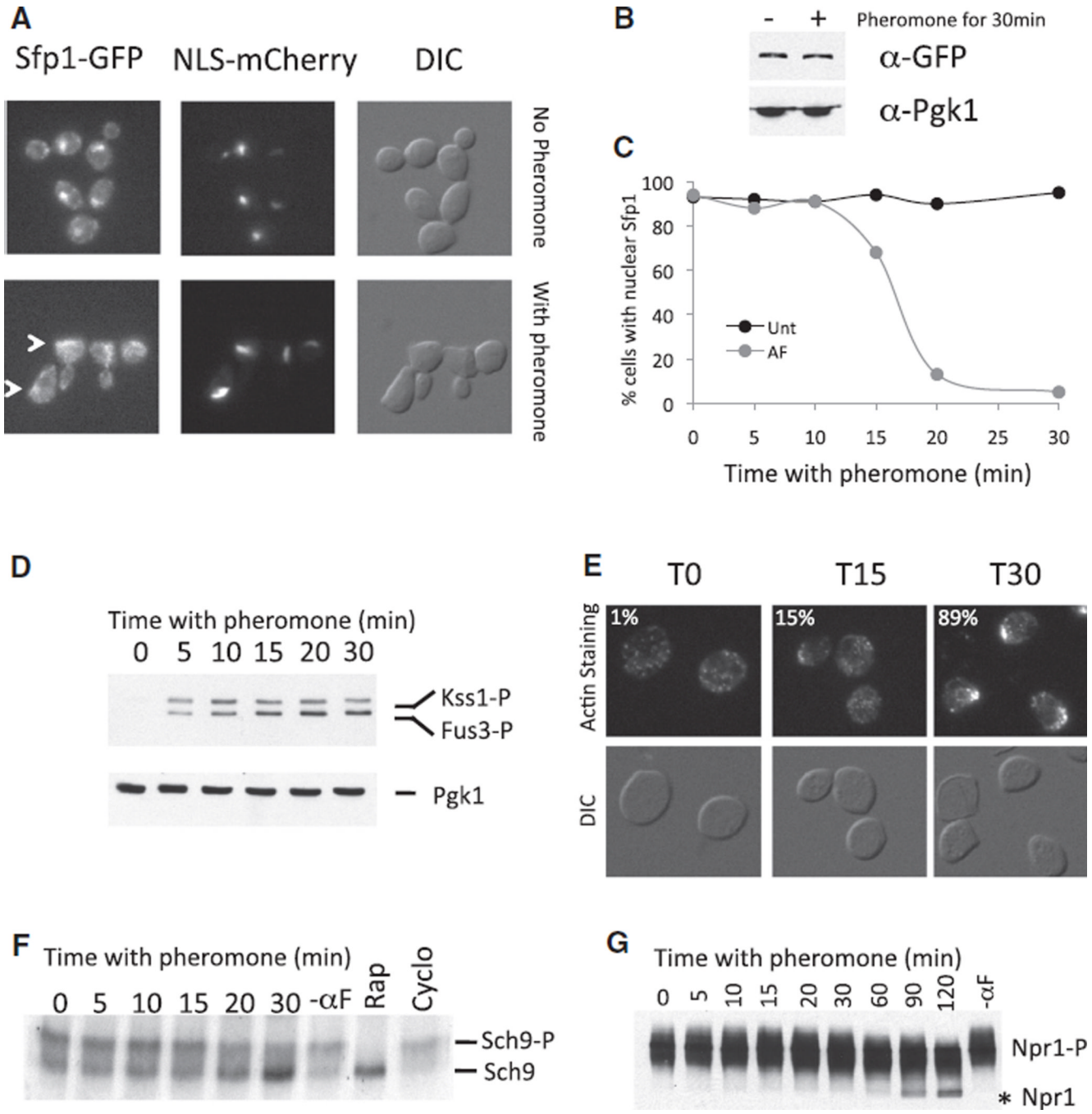

Figure 2. The TORC1 Target Sfp1-GFP Is Exported from the Nucleus after Pheromone Treatment

(A–E) *cdc28-as1 SFP1-GFP NLS-mCherry* cells (A27149) were treated with NM-PP1 (5 μM) for 90 min. Cultures were split and treated as indicated (20 μM pheromone for 30 min; 1 μM rapamycin and 0.33mg/ml cycloheximide for 15 min).

(A) Fluorescence microscopy of cells before (upper panels) or after (lower panels) 30 min of pheromone treatment.

(B) Sfp1-GFP amounts in the presence or absence of pheromone. Pgk1 was used as a loading control.

(C) Quantification of Sfp1-GFP nuclear localization.

(D) MAPK phosphorylation after pheromone treatment. Note that the antibody recognizes both phospho-Fus3 and phospho-Kss1.
(E) Polarization of actin structures was determined by phalloidin staining (n > 100).
(F) *cdc28-as1 SCH9-3HA* cells (A26485) were grown as described in (A) so that the phosphorylation state of Sch9 could be determined.
(G) *cdc28-as1 NPR1-3HA* cells (A23200) were treated with CDK inhibitor (5 μM) split at the time of inhibitor addition and either treated with pheromone (20 μg/ml) or left untreated. An asterisk indicates the hypophosphorylated form of Npr1.

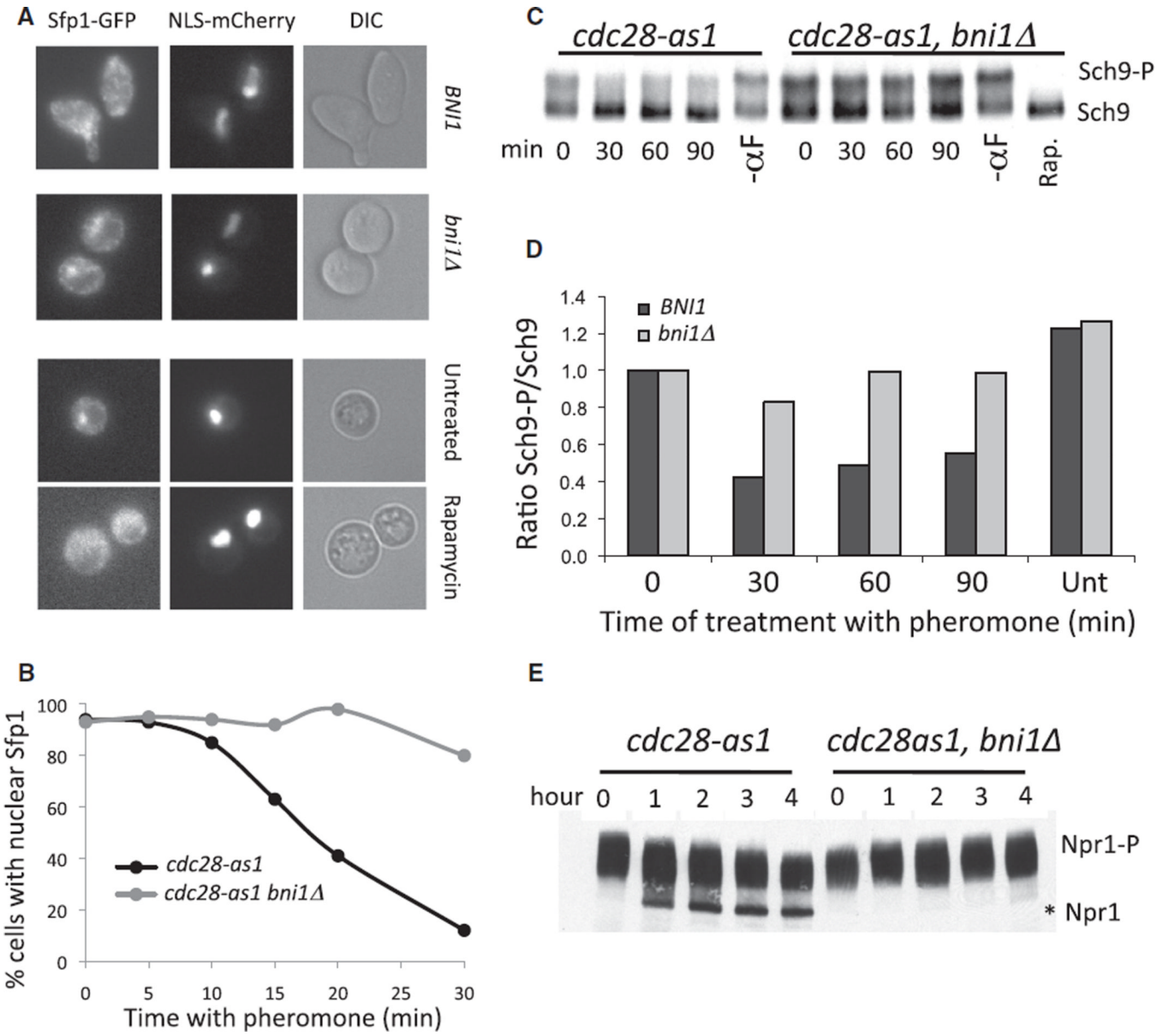

Figure 3. TORC1 Pathway Inactivation by Mating Pheromone Depends on *BNI1*

(A and B) *cdc28-as1* (A27149) and *cdc28-as1 bni1Δ* (A27150) cells were treated as in Figure 2A Sfp1 -GFP and NLS-mCherry were imaged under the indicated conditions. The percent of cells with nuclear Sfp1-GFP localization after pheromone treatment was determined in (B); n = 100.

(C and D) *cdc28-as1* (A26485) and *cdc28-as1 bni1Δ* (A26785) cells were treated as in Figure 2A so that Sch9-3HA phosphorylation could be determined (A). The "-αF" sample was arrested in parallel with the pheromone-treated sample for 120 min. (D) Quantification of the bands shown in (C). Bands were normalized to the 0 min time point.

(E) *cdc28-as1* (A23200) and *cdc28-as1 bni1Δ* (A23441) cells were treated as described in Figure 2A so that Npr1 mobility on SDS PAGE could be examined. The asterisk indicates the position of the hypophosphorylated form of Npr1.

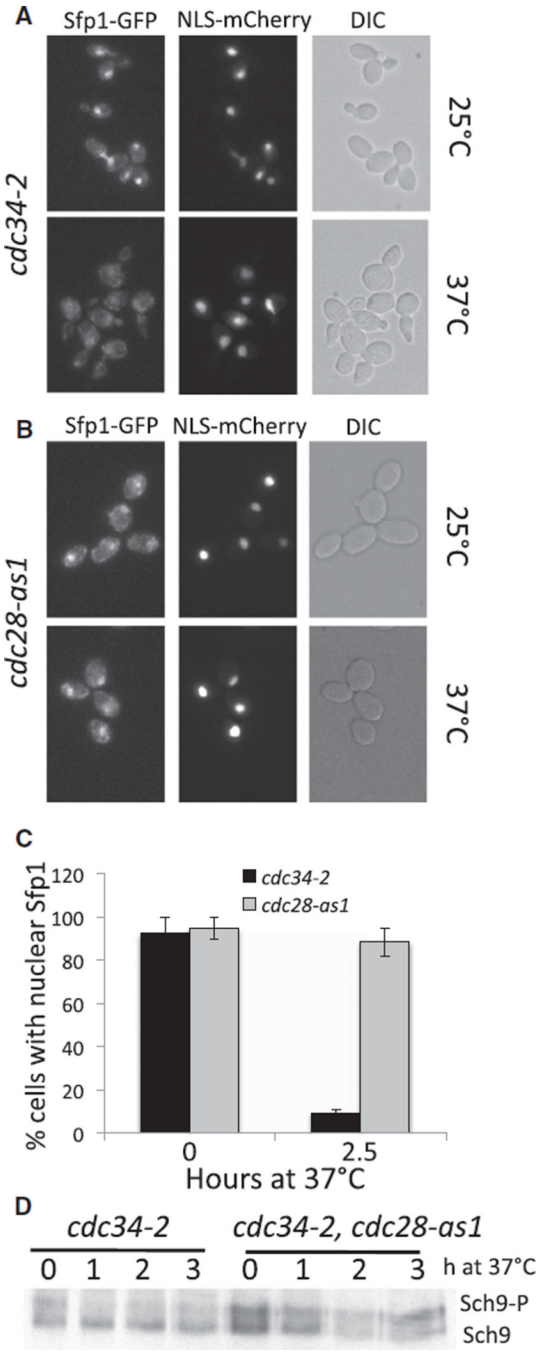

Figure 4. Polarized Growth during Budding Inactivates the TORC1 Pathway

(A–C) *cdc34-2* (A28466) and *cd28-as1* (A27149) were treated with CDK inhibitor (5 μM) and shifted to 37°C for 2.5 hr so that Sfp1 -GFP localization could be determined. Averaged data from at least three independent experiments are plotted in (C) (± standard deviation, n > 100).

(D) *cdc34-2* (A27195) and *cdc34-2 cdc28-as1* (A27196) cells were treated with CDK inhibitor and shifted to 37°C as in (A), and Sch9 mobility was analyzed.

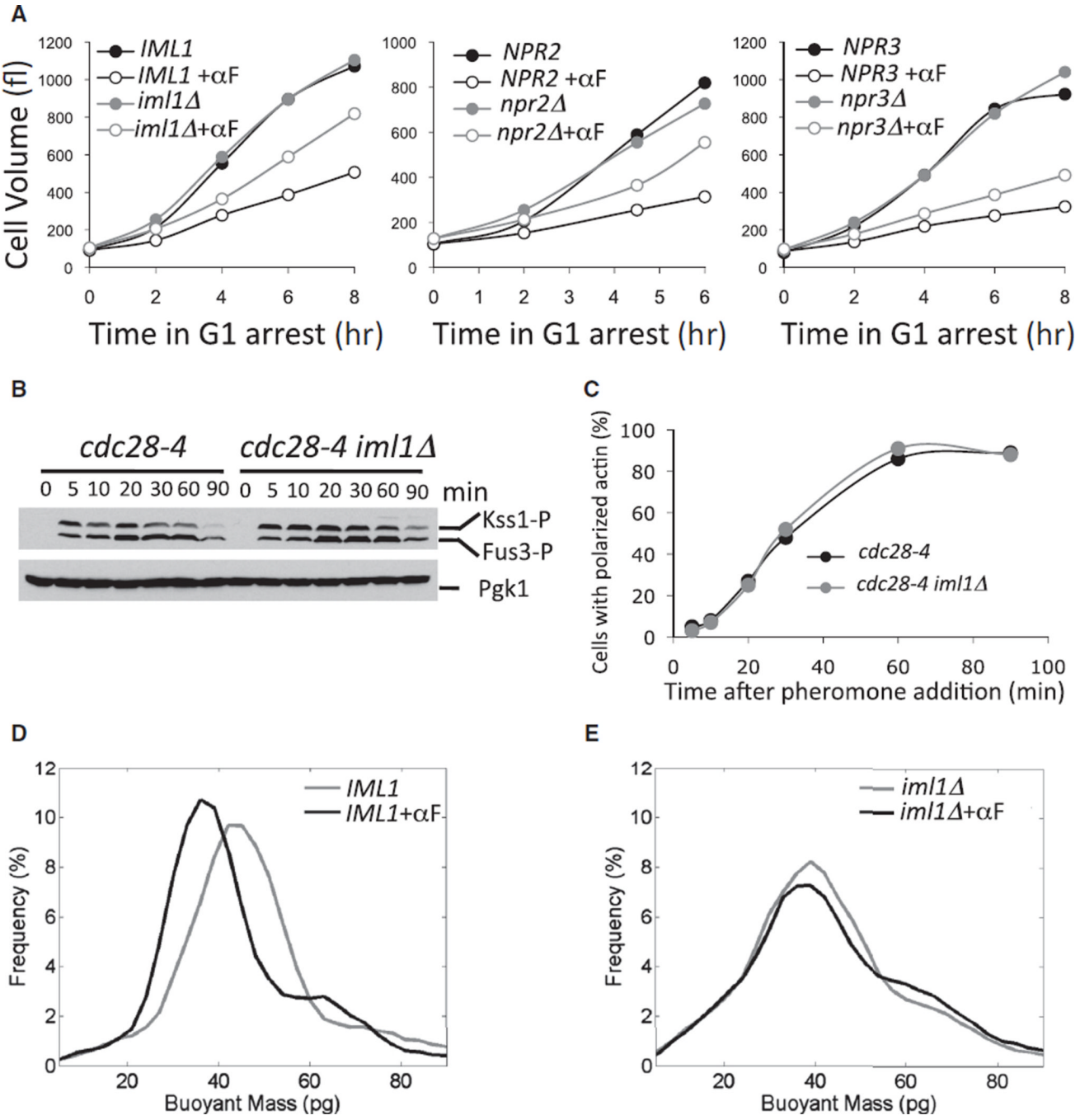

Figure 5. Inactivation of the Iml1 Complex Partially Alleviates the Growth Inhibition Caused by Polarization of the Actin Cytoskeleton

(A) *cdc28-4* (A17132, black symbols), *cdc28-4 iml1*Δ (A33017, gray symbols; left graph), *cdc28-4 npr2*Δ (A31347, gray symbols; middle graph), or *cdc28-4 npr3Δ* (A24515, gray symbols; right graph) cells were shifted to 34°C. One half were treated with pheromone (20 μg/ml, open symbols), and the other half were grown in the absence of pheromone (closed symbols). Cell volume was determined at the indicated times.

(B and C) *cdc28-4* (A17132, black symbols) and *cdc28-4 iml1*Δ (A33017, gray symbols) cells were arrested in G1 for 90 min by incubation at 34°C. Pheromone was added (20 μg/

ml), and Fus3/Kss1 Y-phosphorylation (B) and polarization of the actin cytoskeleton (C; n > 100) were determined.
(D and E) *cdc28-4* (A17132, D) and *cdc28-4 iml1*Δ (A33017, E) cells were shifted to 34°C, and half of the culture was treated with pheromone (20 μg/ml). After 4 hr, buoyant mass was determined.

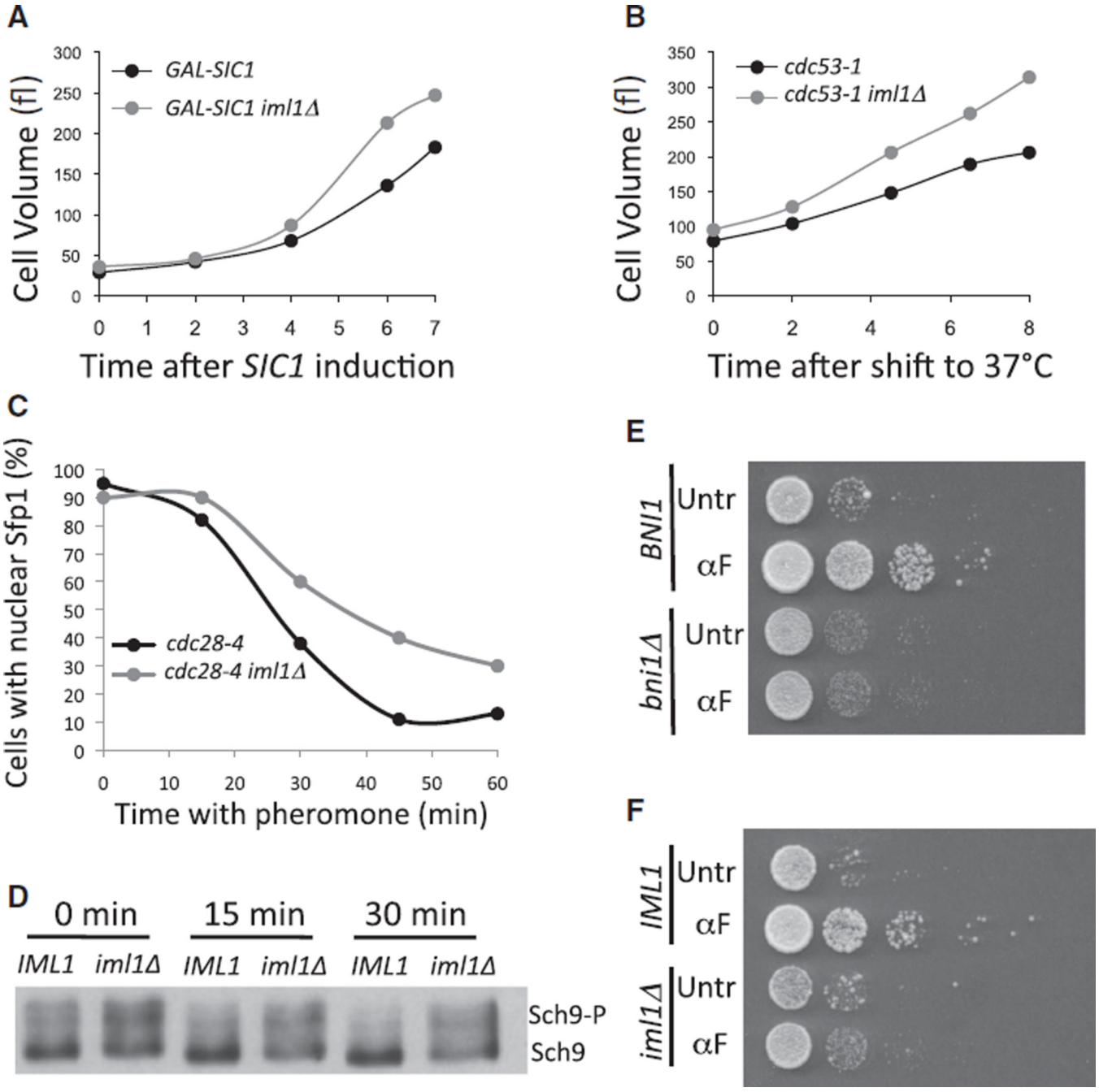

Figure 6. Effects of Unrestrained TORC1 Activity on Polarized Growth and Cell Survival during Prolonged Pheromone arrest

(A) Strains overexpressing *SIC1* and carrying either wild-type *IML1* (A800, black symbols) or an *IML1* deletion (A31265, gray symbols) were grown in YEP + 2% raffinose. At time 0 hr, 1 % galactose was added. Samples were taken at the indicated times so that cell volume could be measured.

(B) *cdc53-1* (A1469, black symbols) and *cdc53-1 iml1*Δ (A30573, gray symbols) cells were shifted to 37°C. Cell size was measured at the indicated times.

(C) *cdc28-4* (A31566, black symbols) or *cdc28-4 iml1Δ* (A31567, gray symbols) cells were arrested in G1 at 34°C for 90 min. At the 0 min time point, cultures were treated with 40 μg/

ml pheromone so that Sfp1-GFP localization could be determined. The increase in the amount of time needed for Sfp1 -GFP to exit the nucleus in this experiment as compared to the times reported in Figure 2C is due to differences in *BAR1* status. *BAR1* strains used here are less sensitive to pheromone than *bar1*Δ strains used in the experiment shown in Figure 2.
(D) *cdc28-4* (A33021) and *cdc28-4 iml1*Δ (A32379) cells were treated as in (C) except that 20 μg/ml pheromone was used. Sch9 mobility was determined at the indicated times.
(E) *cdc28-4* (A17132) and *cdc28-4 bni1*Δ (A18238) were arrested in G1 at 34°C in the absence (Untr) or presence (αF) of pheromone for 6 hr, and 10-fold dilutions were spotted on YPD pates. The plate was scanned after 3 days.
(F) *cdc28-4* (A17132) and *cdc28-4 iml1*Δ (A33017) were grown and treated as in (E).

Table 1

Phosphoproteomic Analysis of Cells with Polarized Actin Cytoskeleton Reveals an Overlap between Rapamycin and Pheromone Treatment

ORF[a]	Protein Name	Regulation by Rapamycin[b]	Regulation by Pheromone[c]	Sites Affected by Pheromone[d]
YBL054W	Tod6	down	NA	
YBL103C	Rtg3	down	<1.5-fold	S455
YDR005C	Maf1	down	NA	
YDR169C	Stb3	down	up	S9
YER040W	Gln3	down	down and up	down S276, S287; up S689
YFL021W	Gat1	down	up	S300, T369
YER169W	Rph1	up	up	S412, S430, S552, S561, S698
YIL038C	Not3	down	down	S344, T440, S442, S446, S450, T454, T555, S565, S569, T571
YER088C	Dot6	down	down	S553
YBR181C	Rps6b	down and up	up	Y7
YGR162W	Tif4631	down	up	S176, S213, T276, T442
YOR204W	Ded1	up	down	S576
YPL090C	Rps6a	down and up	NA	
YPR041W	Tif5	up	up	S170, S189, T317
YDR028C	Reg1	down	up	T286, S344, S429, S773, S778, Y780
YHR082C	Ksp1	down	down	S416, S419, T521, S529
YHR205W	Sch9	down	down	S723
YNL183C	Npr1	down	down	S241
YMR216C	Sky1	down	down and up	down S360, S453; up T66
YNL076W	Mks1	down	<1.5-fold	
YPL180W	Tco89	down	down and up	down S104, S267, S288, S575; up S255
YPR185W	Atg13	down	down	S454, S461, S652, S656
YDR345C	Hxt3	down	up	S3
YJR001W	Avt1	down	NA	
YNL321W	Vnx1	up	up	T26, S110, S121
YML035C	Amd1	down	down	S105
YMR205C	Pfk2	up	up	S41, S42, S170
YOL061W	Prs5	up	down	S325
YBL051C	Pin4	up	up	T465, S466
YCL011C	Gbp2	down and up	NA	
YCR077C	Pat1	down	up	S279, S457
YDL051W	Lhp1	up	NA	
TDL173W	Par32	up	down and up	down S241, S249, S250; up S36
YDR348C		down	NA	
YIL047C	Syg1	down	NA	
YIL135C	Vhs2	down	<1.5-fold	
YLR257W		up	up	S129, T159, S197
YMR196W		up	up	S984, S1081

ORF[a]	Protein Name	Regulation by Rapamycin[b]	Regulation by Pheromone[c]	Sites Affected by Pheromone[d]
YMR275C	Bul1	up	up	S252
YNL004W	Hrb1	down and up	up	S355
YNL265C	Ist1	down	NA	
YOL060C	Mam3	down	down and up	down S614, T617; up S439
YOR322C	Ldb19	up	NA	

[a] Yeast cells were arrested inG1 with or without pheromone. Total protein was extracted, labeled, and processed by mass spectometry and phospho-mass spectometry. The complete data set is shown in Table S1. Genes are ordered by functional categories as previously presented [29].

[b] Indicates whether a protein was dephosphorylated (down) or phosphorylated (up) after rapamycin treatment as reported in [29].

[c] Indicates whether at least a single phospho peptide within that protein changed abundance more than 1.5-fold between samples with or without pheromone. “up” or “down” denote phosphorylation and dephosphorylation, respectively. NA indicates that no phospho peptides were recovered.

[d] Sites that are affected at least 1.5-fold in the indicated direction. Underlined sites were also reported as rapamycin sensitive [29].